# NANOFLUID FLOW COMPRISING GYROTACTIC MICROBES THROUGH A POROUS MEDIUM - A NUMERICAL STUDY

by

***Sohail AHMAD[a], Muhammad ASHRAF [a*] and Kashif ALI[b]***

[a]Centre for Advanced Studies in Pure and Applied Mathematics, Bahauddin Zakariya University, Multan, Pakistan.

[b]Department of Basic Sciences and Humanities, Muhammad Nawaz Sharif University of Engineering and Technology, Multan, Pakistan.

**Abstract**

*Researchers have significantly contributed to heat transfer field and always made out much effort to find new solutions of heat transfer augmentation. In the concerned work, we have presented a novel study regarding heat and mass transfer flow of nanofluid in the presence of gyrotactic microbes through a porous medium past a stretching sheet. The nonlinear coupled ODEs are obtained after applying the persuasive tool of similarity transformation on governing model PDEs and then tackled numerically by exploiting the SOR (Successive over Relaxation) parameter method. The outcomes of assorted parameters for the flow are surveyed and discussed through graphs and tables. A graphical comparison is correlated with previously accomplished study and examined to be in an exceptional agreement. The culminations designate that the bioconvection Peclet number and microorganism concentration difference parameter enhance density of the motile microorganisms. Moreover, porosity parameter substantially increases shear stress on sheet surface. The addition of nanoparticles in microorganisms is beneficial to improvise the thermal efficiency of many systems like bacteria powered micro-mixers, microfluidics devices like micro-volumes and enzyme biosensor, microbial fuel cells and bio-microsystems like chip-shaped microdevices.*

Keywords: *Nanofluid, gyrotactic microorganisms, heat transfer, Concentration, SOR*

## Introduction

In new era of research, the novel study of boundary layer nanofluid flow enclosing gyrotactic microorganisms (microbes) with mass and heat transfer over a stretching surface has got a valuable attention among research community and scientists because of its abundant practical implementations in various fields of science and bio-technology. The advantages of adding mobile microbes to the nanoparticles suspension involve improved nanofluid stability, microscale mixing, enhanced mass transfer and use in microvolumes [1]. There is potential of employing nanofluids with microbes in

* Corresponding author E-mail: muhammadashraf@bzu.edu.pk

several bio-microsystems like chip-shaped microdevices to evaluate toxicity of nanoparticles, the optimization of celluloses production and provocative response of the lung to silica nanoparticles [2, 3]. Phycocolloides like alginic acid and carrageenan are primarily constituents of brown and red algal cell walls and are used in industry such as crude oil and natural gas production [4]. The gyrotactic microbes are also helpful to enhance nanofluids stability [5]. Microbial-enhanced oil recovery is also application of bioconvection phenomena where nutrients and microbes are inserted in oil bearing layer to maintain the variation in permeability [6].

Recently, the intention of research scholars is diverted towards flow of nanofluids enfolding gyrotactic microbes. Kuznetsov [7] commenced the abstract work of bioconvection nanofluid incorporating gyrotactic microorganisms and declared that the self-propelled motile microbes strengthen mixing and avert nanoparticles accumulation in nanofluids. The problems of nanofluids and gyrotactic microbes have been examined theoretically, experimentally and numerically by several authors. Ramzan et al. [8] analyzed the mass and heat transfer in both nanofluid and gyrotactic microorganisms. This study included viscous dissipation with convective boundary conditions, non-linear thermal radiation and slip effects. It was observed that microorganisms motile density declines with climbing values of Lewis and Peclet numbers. In an investigation on nanofluid flow comprising gyrotactic microorganisms under the impact of external magnetic field by Chakraborty [9], it was noticed that the heat transport rate, momentum boundary layer thickness and the flux rate of motile microorganisms across the fluid medium diminish with an increment in the magnetic field parameter while the nanoparticle concentration enhanced. Rashidi et al. [10] examined the effect of solid surface structure on the condensation flow of Argon in rough nanochannels with different roughness geometries using molecular dynamics simulation. Rashad et al. [11] investigated the effect of magnetic field and internal heat generation on the free convection flow in a rectangular cavity filled with a porous medium saturated with Copper water nanofluid. It was found that the average Nusselt number decreases as the Hartmann number or the solid volume fraction increases. The stratified bioconvective nanofluid flow was considered by Alsaedi et al. [12]. The nanofluid flow in the presence of magnetohydrodynamics and gyrotactic microorganisms propagating over a stretching/shrinking surface was analyzed by Shahid et al. [13]. Non-dimensional variables were employed to simplify the governing equations and then the obtained coupled ODEs were solved numerically by applying "Successive Taylor Series Linearization Method (STSLM)". This research explained how the magnetic field and radiation boost up the temperature and velocity of the fluid. Aziz et al. [14] worked on the bioconvective nanofluid boundary layer flow and reported that the propagation rate of motile microorganisms is marginally affected by bioconvection parameters. Numerical study of natural convection heat transfer of a nanofluid in an L-shaped enclosure with a heating obstacle was presented by Mohebbi and Rashidi [15]. The maximum Nusselt number was observed when the heating obstacle was located in the lower position inside the left wall of L-shaped enclosure. It was found by Shen et al. [16] that the density of the gyrotactic microorganisms strongly depends on the bioconvection parameters. Numerical investigations of some fluid flows past through porous medium can be studied in the articls by Ahmad et al. [17-20].

All types of fluid flows through porous media usually exists in scientific and technological fields and its theory has been successfully used in the fields such as, geothermal and petroleum engineering, micro machines, chemical industry, mineral engineering, soil mechanics and so on. Numerically, no enough study on the flow of nanofluids comprising gyrotactic microbes through porous medium has

been found in literature. The main purpose of studying this paper is to examine the novel results, achieved during the analysis of nanofluid flow through a porous medium containing nanoparticles and gyrotactic microbes. Pertinent results, obtained under various situations arose by varying the governing parameters, are discussed and envisioned through graphs and tables.

## Description of Mathematical Model

We assume two-dimensional and steady nanofluid flow through a porous medium enclosing both the gyrotactic microbes and nanoparticles. $u_e(x) = ax^m$ is to be taken as an ambient velocity and that of $u_w(x) = cx^m$ is stretching velocity, where $m$ is positive constant other than one (due to nonlinear stretching sheet). In addition, $N_w$, $C_w$ and $T_w$ are taken as the concentration of the microorganisms, concentration and temperature of fluid at the sheet surface. It is supposed that the velocity of swimming microbes as well as swimming path way do not possess any change in the presence of nanoparticles. This assumption is valid only if concentration of nanoparticles is below than 1%. Thereby, bioconvection stability can be acquired by mixing solid nano particles alongwith microbes in the liquid (base fluid). Momentum, species and thermal boundary layers across the flow region are shown in the flow sketch fig. 1.

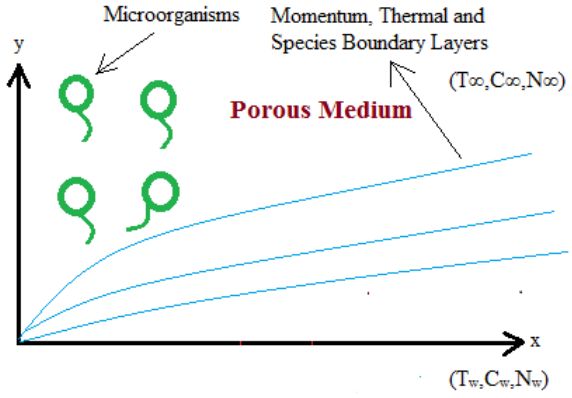


**Figure 1. Geometry of the Flow Problem.**

The model boundary layer equations, in case of porous medium, can be formulated as [13, 18]:

$$\frac{\partial v}{\partial y} + \frac{\partial u}{\partial x} = 0 \tag{1}$$

$$u\frac{\partial u}{\partial x} + v\frac{\partial u}{\partial y} = \upsilon\frac{\partial^2 u}{\partial y^2} + u_e\frac{\partial u_e}{\partial x} + \frac{\mu}{\rho k^*}\left(u_e - u\right) \tag{2}$$

$$u\frac{\partial T}{\partial x} + v\frac{\partial T}{\partial y} = \frac{\tau D_T}{T_\infty}\left(\frac{\partial T}{\partial y}\right)^2 + \tilde{\beta}\frac{\partial^2 T}{\partial y^2} + \tau D_B\frac{\partial C}{\partial y}\frac{\partial T}{\partial y} \tag{3}$$

$$v\frac{\partial C}{\partial y} + u\frac{\partial C}{\partial x} = D_B\frac{\partial^2 C}{\partial y^2} + \frac{D_T}{T_\infty}\frac{\partial^2 T}{\partial y^2} \tag{4}$$

$$v\frac{\partial N}{\partial y} + u\frac{\partial N}{\partial x} + \frac{1}{C_w - C_\infty}\frac{\partial}{\partial y}\left[N\left(\frac{\partial C}{\partial y}\right)\right]bW_c = D_n\frac{\partial^2 N}{\partial y^2} \tag{5}$$

where $(x, y)$ being the coordinates along and normal to the sheet with $u$ and $v$ being the respective velocity components in these directions. The pressure term $-\frac{1}{\rho}\frac{\partial p}{\partial x}$ in momentum equation (2) has been adjusted by $u_e \frac{\partial u_e}{\partial x}$ using Bernoulli equation. The analogous Boundary Conditions (BCs) are:

$$u = cx^m,\ N = N_w,\ C = C_w,\ T = T_w,\ v = v_w(x) \qquad \text{at } y = 0 \tag{6}$$

$$u = ax^m,\ N = N_\infty,\ C = C_\infty,\ T = T_\infty \qquad \text{at } y \to \infty \tag{7}$$

$v_w$ is mass flux which corresponds to suction $(v_w > 0)$ and injection $(v_w < 0)$.

Following similarity transformations are introduced along with stream function to transmute the governing PDEs (2)-(5) into ODEs.

$$\psi = \sqrt{ax^{m+1}\upsilon}\, f(\eta),\ \eta = \sqrt{\frac{a}{\upsilon}x^{m-1}}\, y,\ G(\eta) = \frac{N - N_\infty}{N_w - N_\infty},\ \phi(\eta) = \frac{C - C_\infty}{C_w - C_\infty},\ \theta(\eta) = \frac{T - T_\infty}{T_w - T_\infty} \tag{8}$$

Entreating these variables in eqs. (2)-(5), we acquire the following set of equations:

$$f''' + P_0\left(1 - f'\right) = m\left(-1 + f'^2\right) - \frac{1+m}{2} ff'' \tag{9}$$

$$\frac{1}{\Pr}\theta'' + N_b\phi'\theta' + \frac{1+m}{2} f\theta' + N_t\theta'^2 = 0 \tag{10}$$

$$\phi'' - Le\phi = -\frac{N_t}{N_b}\theta'' - \frac{1+m}{2} Lef\phi' \tag{11}$$

$$G'' + \frac{1+m}{2} ScfG' = Pe\left[\phi'G' + \left(G + \Omega\right)\phi''\right] \tag{12}$$

The interrelating BCs are:

$$\eta = 0:\ f = S,\ f' = \alpha,\ \phi = 1,\ G = 1,\ \theta = 1 \qquad \eta \to \infty:\ \phi \to 0,\ f' \to 1,\ \theta \to 0,\ G \to 0 \tag{13}$$

where $\alpha$ is the stretching of sheet parameter, $S$ is suction/injection and the other dimensionless parameters involved in the system of eqs. (9)-(12) are:

$$\left.\begin{aligned} P_0 &= \frac{\nu x}{k^* u_e}, & N_b &= \frac{\tau D_B\left(C_w - C_\infty\right)}{\nu}, & \Omega &= \frac{N_\infty}{N_w - N_\infty}, & Sc &= \frac{\nu}{D_n}, \\ Le &= \frac{\nu}{D_B}, & N_t &= \frac{\tau D_T\left(T_w - T_\infty\right)}{\nu T_\infty}, & \Pr &= \frac{\nu}{\alpha}, & Pe &= \frac{bW_c}{D_n} \end{aligned}\right\} \tag{14}$$

Here $P_0$ signifies the porosity parameter, $N_b$ refers to the parameter of Brownian motion, $\Omega$ is recognized as motile microorganism parameter, $Sc$ conveys the bioconvection Schmidt number, $Le$ stands for Lewis number, $N_t$ denotes the thermophoresis parameter, $\Pr$ exemplifies the Prandtl number and $Pe$ indicates the Peclet number. The quantities of engineering interest in dimensionless form like local Sherwood number $Sh_x$, local density number of motile microorganism $Nn_x$, skin friction $C_{fx}$ and Nusselt number $Nu_x$ may be defined as:

$$\mathrm{Re}_x^{-\frac{1}{2}} Sh_x = -\phi'(0),\quad \mathrm{Re}_x^{-\frac{1}{2}} Nn_x = -G'(0),\quad \mathrm{Re}_x^{\frac{1}{2}} C_{fx} = f''(0),\quad Nu_x\, \mathrm{Re}_x^{-\frac{1}{2}} = -\theta'(0) \tag{15}$$

whereas $\mathrm{Re}_x = U_e x/\nu$ denotes the local Reynolds number.

## Numerical Solution using SOR Method

Sometimes, the algorithms (for numerical simulation) become unstable for dynamical problems even for very precise guesses of boundary conditions. This anomaly may be due to the implicit dependency of the solution on original initial conditions and instability of the differential equations. That is why we require some persuasive approach, which can tackle all complexities. Some other multi-step and implicit methods can also be employed to solve the dynamical problems of such type (as in the present case). But, these methods may take enormous computation time. However, we adopt an alternate approach based on the finite difference discretization of ODEs. A finite difference methodology may not suffer from these shortcomings. Therefore, our previous work (please see Ashraf et al. [21-23]) involved an approach (SOR) based on finite difference method.

However, exploiting the SOR method one can overcome such type of difficulties. We construct numerical algorithm of our problem at a specific grid point $\eta = \eta_i$ by compensating the derivatives with central differences, and then the subsequent system is iteratively solved with the help of Successive over Relaxation (SOR) method along with BCs. The SOR method is a well renowned scheme to find the approximate solutions of nonlinear differential equations with very quick convergence. One seeks value of the relaxation parameter (extrapolation factor) that accelerates the iteration procedure for which the SOR method converges.

We recede the order of eq. (9) by one after substituting:

$$s = f' = \frac{df}{d\eta} \tag{16}$$

so that, we have to solve the nonlinear eqs. (9)-(12) in the form:

$$s'' + P_0\left(1-s\right) = m\left(-1+s^2\right) - \frac{1+m}{2} fs' \tag{17}$$

$$\frac{1}{\Pr}\theta'' + N_b\phi'\theta' + \frac{1+m}{2} f\theta' + N_t\theta'^2 = 0 \tag{18}$$

$$\phi'' - Le\phi = -\frac{N_t}{N_b}\theta'' - \frac{1+m}{2} Lef\phi' \tag{19}$$

$$G'' + \frac{1+m}{2} ScfG' = Pe\left[\phi'G' + \left(G+\Omega\right)\phi''\right] \tag{20}$$

with BCs:

$$f(0)=1,\ s(0)=\alpha,\ s(\infty)=1,\ \theta(0)=1,\ \theta(\infty)=0,\ G(0)=1,\ G(\infty)=0,\ \phi(0)=1,\ \phi(\infty)=0. \tag{21}$$

After applying finite differences, eqs. (17)- (20) take the form:

$$\hat{s}_i = \frac{1}{A_1}\left(B_1\hat{s}_{i+1} + C_1\hat{s}_{i-1} + D_1\right) \tag{22}$$

$$\hat{\theta}_i = \frac{1}{A_3}\left(B_3\hat{\theta}_{i+1} + C_3\hat{\theta}_{i-1} + D_3\right) \tag{23}$$

$$\hat{\phi}_i = \frac{1}{A_4}\left(B_4\hat{\phi}_{i+1} + C_4\hat{\phi}_{i-1} + D_4\right) \tag{24}$$

$$\hat{G}_i = \frac{1}{A_2}\left(B_2\hat{G}_{i+1} + C_2\hat{G}_{i-1} - D_2\right) \tag{25}$$

where

$$A_1 = 4 + 2h^2 P_0 + 2h^2 m\bar{s}_i,\ B_1 = \frac{1+m}{2} hf_i + 2,\ C_1 = 2 - \frac{1+m}{2} hf_i,\ \ D_1 = 2h^2 m + 2h^2 P_0$$

$$A_2 = \frac{8}{\Pr},\quad B_2 = \frac{4}{\Pr} + N_b\left(\hat{\phi}_{i+1} - \hat{\phi}_{i-1}\right) + (1+m)hf_i + N_t\hat{\theta}_{i+1} - 2N_t\hat{\theta}_{i-1},\quad C_2 = \frac{4}{\Pr} - N_b\left(\hat{\phi}_{i+1} - \hat{\phi}_{i-1}\right)$$

$$-(1+m)hf_i + N_t\hat{\theta}_{i-1},\quad D_2 = 0,\quad A_3 = 4 + 2h^2 Le,\ \ B_3 = 2 + \frac{1+m}{2} Lehf_i,\quad C_3 = 2 - \frac{1+m}{2} Lehf_i, \tag{26}$$

$$D_3 = 2\frac{N_t}{N_b}\left(\hat{\theta}_{i+1} + \hat{\theta}_{i-1} - 2\hat{\theta}_i\right), A_4 = 4 + 2Pe\left(\hat{\phi}_{i+1} + \hat{\phi}_{i-1} - 2\hat{\phi}_i\right), B_4 = 2 + \frac{1+m}{2} hScf_i - \frac{Pe}{2}\left(\hat{\phi}_{i+1} - \hat{\phi}_{i-1}\right),$$

$$C_4 = 2 - \frac{1+m}{2} hScf_i + \frac{Pe}{2}\left(\hat{\phi}_{i+1} - \hat{\phi}_{i-1}\right), D_4 = -2Pe\,\Omega\left(\hat{\phi}_{i+1} + \hat{\phi}_{i-1} - 2\hat{\phi}_i\right)$$

whereas $h$ embodies the grid length. The algebraic system of nonlinear eqs. (17)- (20) is solved repetitively, with respect to the BCs (21), by SOR method. To make better exactness of the numerical solution and for an appropriate decision of the estimations of the framework, we ratify the following criteria.

- The solution of eqs. (22)- (25) is determined with the help of SOR method subject to the last eight conditions in (21).
- New guess $\hat{f}^{(k+1)}$ for the solution of eq. (16) is processed, subject to the first condition given in (21), by Simpson's rule which is then utilized to determine $\hat{s}^{(k+1)}$ in eq. (22).
- For the convergence test $\hat{s}^{(k+1)}, \hat{\theta}^{(k+1)}, \hat{G}^{(k+1)}, \hat{\phi}^{(k+1)}$ and $\hat{f}^{(k+1)}$ are calculated along with $\hat{s}^{(k)}$, $\hat{\theta}^{(k)}, \hat{G}^{(k)}, \hat{\phi}^{(k)}$ and $\hat{f}^{(k)}$.

The iterative process is continued as far as:

$$\max\left[\|\hat{s}^{(k+1)} - \hat{s}^{(k)}\|_{L_2}, \|\hat{\theta}^{(k+1)} - \hat{\theta}^{(k)}\|_{L_2},\ \|\hat{G}^{(k+1)} - \hat{G}^{(k)}\|_{L_2}, \|\hat{\phi}^{(k+1)} - \hat{\phi}^{(k)}\|_{L_2}, \|\hat{f}^{(k+1)} - \hat{f}^{(k)}\|_{L_2}\right] < TOL_{iter}$$

For all the calculations performed here, the value of $TOL_{iter}$ is taken at least $10^{-11}$.

## Results and Discussion

The nonlinear governing eqs. (17)-(20) are solved numerically subject to the BCs (21) by means of a finite-difference based technique known as the SOR method, as described in the book by Hildebrand FB [24], for a variety of estimated values of the governing parameters e.g. $P_0, m, \Pr, N_b, N_t, Le, Sc, Pe, \Omega$ and $\alpha$. The step size of $\eta$ as well as the edge of the boundary layer are balanced in such a way that the velocity $F'(\eta)$, temperature $\theta(\eta)$, concentration $\phi(\eta)$ and motile density distribution $G(\eta)$ show asymptotic demeanor for various scopes of physical parameters. Some of the parametric values are assumed fixed e.g. $P_0 = 0.6, Sc = 1.5, Pe = 0.4, \Omega = 0.2$ and $\alpha = 0.5$ otherwise specified in graphs. Following Rashidi et al. [25], we have taken value of the Prandtl as $\Pr = 6.2$ which is fixed in all the calculations performed here.

While observing the velocity distribution for $\alpha = -1$ (shrinking of sheet case) and various values of the positive constant $m$ by taking $P_0 = 0$, it is examined that the velocity profile rises up in the flow region with an increase in the values of $m$. The same trend, for velocity profile, was noticed by Shahid et al. [13] as envisioned in fig. 2.

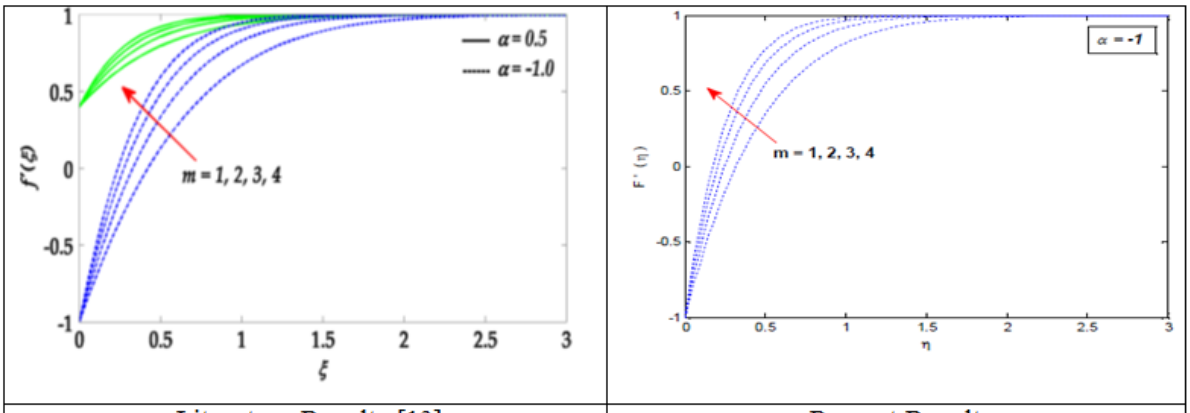


Literature Results [13] | Present Results

**Figure 2. Impact of $m$ on velocity distribution for $\alpha = -1$.**

From tab. 1, it is obvious that the impact of positive constant $m$ and the porosity parameter $P_0$ is to escalate the skin friction coefficient while $m$ also strengthens heat transport rate as well as motile microorganisms density but downturns mass transfer rate. It is noted from tab. 2 that the Prandtl number $\Pr$ improves the heat transfer rate however $N_t$ (thermophoresis parameter) reduces it. Moreover, the values of the Sherwood number $Sh_x$ boost up with rising values of the Brownian parameter $N_b$ and these values also elevate with the influence of the Lewis number $Le$ as envisioned in tab. 3.

**Table 1. $C_{fx}$, $Nu_x$, $Sh_x$ & $Nn_x$ for various $m$ and $C_{fx}$ for various $P_0$**

| $m$ | $C_{fx}$ | $-Nu_x$ | $-Sh_x$ | $-Nn_x$ | $P_0$ | $C_{fx}$ |
|---|---|---|---|---|---|---|
| 1 | 1.11823 | 2.58004 | 0.35553 | 2.06672 | 11 | 2.34573 |
| 2 | 1.52348 | 3.89841 | 0.14013 | 2.75043 | 22 | 2.94665 |
| 3 | 1.88571 | 5.23386 | -0.12661 | 3.39717 | 33 | 3.43161 |
| 4 | 2.22361 | 6.58065 | -0.42367 | 4.02287 | 44 | 3.84913 |
| 5 | 2.54565 | 7.93473 | -0.73914 | 4.63636 | 55 | 4.22113 |

**Table 2. $Nu_x$ for various $Pr$ & $N_t$**

| Pr | $-Nu_x$ | $N_t$ | $-Nu_x$ |
|---|---|---|---|
| 1 | 1.85882 | 0.0 | 5.59169 |
| 3 | 3.51009 | 0.3 | 3.89841 |
| 5 | 4.65630 | 0.6 | 2.72824 |
| 7 | 5.58816 | 0.9 | 1.94918 |
| 10 | 6.76289 | 1.2 | 1.43349 |

**Table 3. $Sh_x$ for various $N_b$ & $Le$**

| $N_b$ | $-Sh_x$ | $Le$ | $Sh_x$ |
|---|---|---|---|
| 0.2 | 0.53434 | 0.2 | 0.06582 |
| 0.3 | 1.85504 | 0.4 | 0.72884 |
| 0.5 | 2.85262 | 0.6 | 1.22157 |
| 0.8 | 3.32939 | 0.8 | 1.62587 |
| 1.5 | 3.55068 | 1.0 | 1.98544 |

**Table 4. $Nn_x$ for various $S_c$, $Pe$ & $\Omega$**

| $S_c$ | $-Nn_x$ | $Pe$ | $-Nn_x$ | $\Omega$ | $-Nn_x$ |
|---|---|---|---|---|---|
| 0.2 | 0.21459 | 0.1 | 3.26803 | 0.0 | 3.14259 |
| 0.4 | 0.69014 | 0.2 | 2.99092 | 0.1 | 3.08887 |
| 0.6 | 1.13785 | 0.3 | 2.71386 | 0.3 | 2.98142 |
| 0.8 | 1.57117 | 0.4 | 2.43680 | 0.5 | 2.87398 |
| 1.0 | 1.99578 | 0.5 | 2.15969 | 0.7 | 2.76653 |

The bioconvection Schmidt number $S_c$ increases the density $Nn_x$ of the motile microorganisms while the Peclet number $Pe$ and the microorganism concentration difference parameter $\Omega$ reduce $Nn_x$, as predicted in tab. 4. It is noticed here that the porous medium enhances the shear stress and that of bioconvection parameters ($Pe$ and $\Omega$) tend to decrease the density of the motile microorganisms respectively. It is seen that the rate of mass transfer grows with Brownian motion parameter and the rate of heat transfer drops with the effect of thermophoretic parameter.

Figures 3 and 4 describe the demeanor of velocity and motile microorganisms density profiles for multiple values of $m$. The profile $F'(\eta)$ rises up whereas the profile $G(\eta)$ across the boundary layer shows a decreasing trend with $m$. The stretching of sheet parameter $\alpha$ is subsidized to accelerate the flow velocity that can be observed from fig. 3. Furthermore, $\alpha > 0$ denotes the stretching of sheet, $\alpha < 0$ corresponds to the shrinking case, $\alpha = 1$ describes no boundary layer and $\alpha = 0$ is correlated with the planar stagnation point flow.

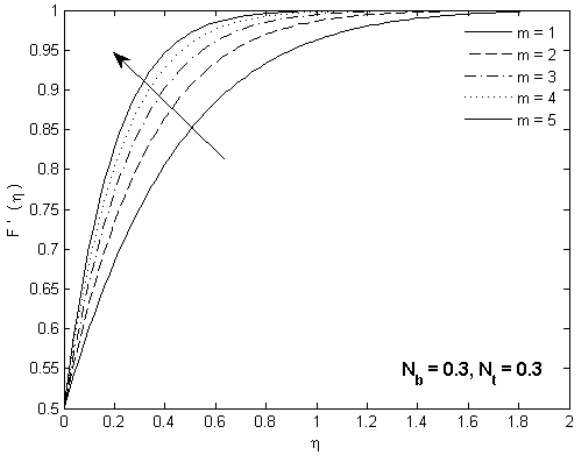


**Fig. 3. Velocity profile for various $m$.**

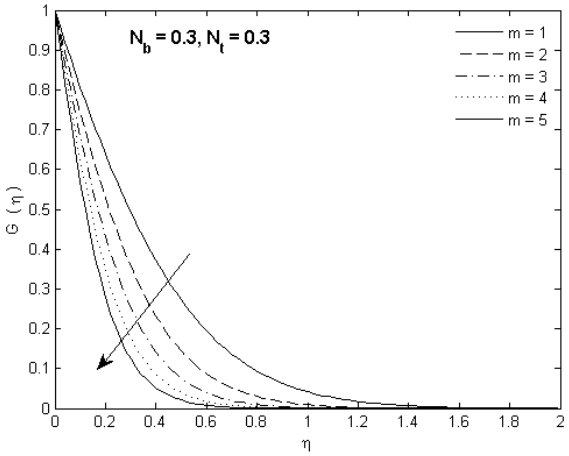


**Fig. 4. Motile microorganisms density profile for various $m$.**

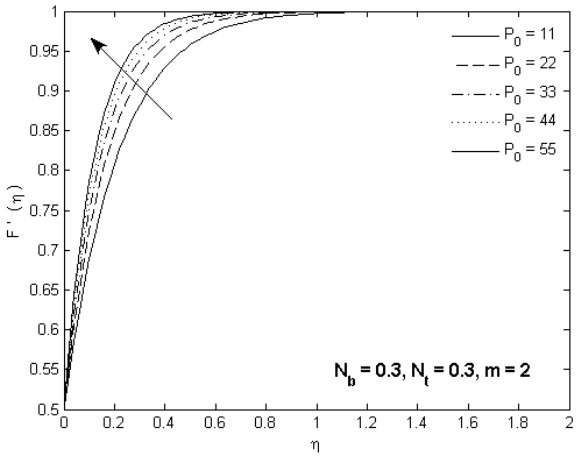


**Fig. 5. Velocity profile for various $P_0$.**

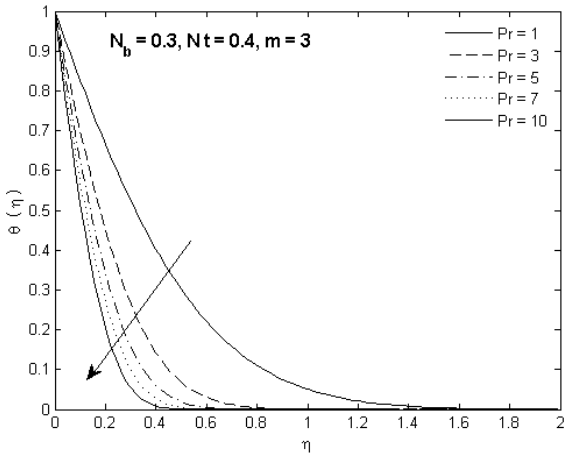


**Fig. 6. Temperature profile for various $Pr$.**

Figure 5 reveal the impact of the porosity parameter $P_0$ on streamwise velocity profile. An increment in the values of $P_0$ marginally boosts the magnitude of the velocity**.** It is also observed here

from fig. 6 that the Prandtl number substantially reduces the temperature profile and the thermal boundary layer thickness becomes thinner while an opposite trend, as compared with $\Pr$, is noted in case of the thermophoresis parameter (see fig. 7). The force induced by the thermophoresis has competency to shift the particles from hotter to cooler area. Furthermore, if the fluid comprehends the high Prandtl number then its temperature drops down.

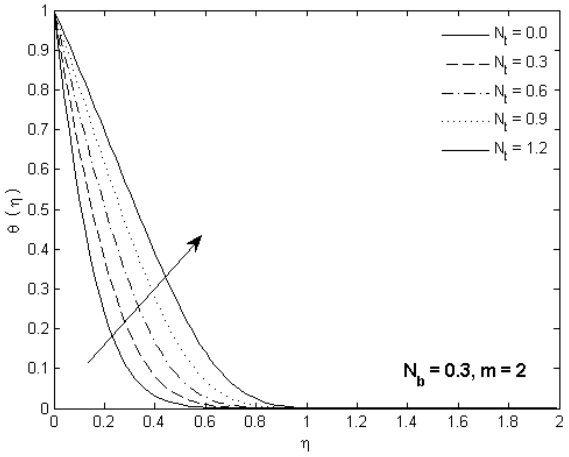


**Fig. 7. Temperature profile for various $N_t$.**

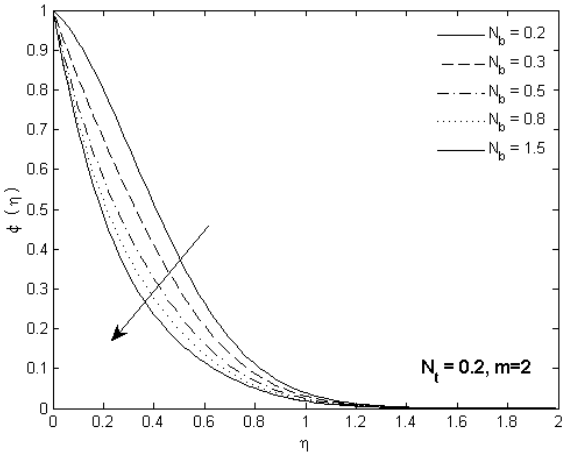


**Fig. 8. Concentration profile for various $N_b$.**

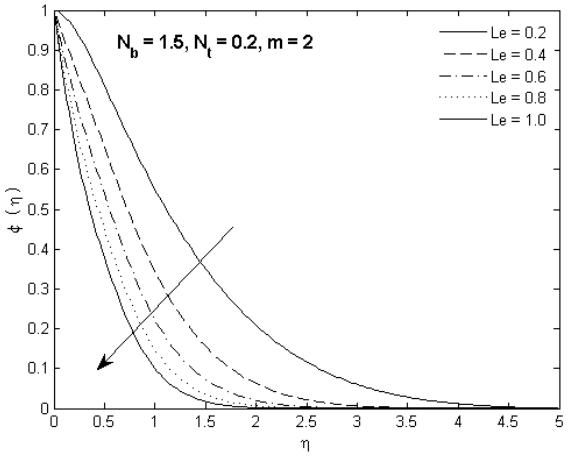


**Fig. 9. Concentration profile for various $Le$.**

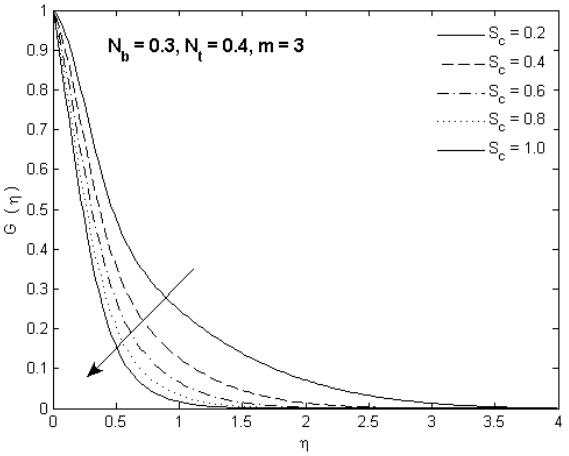


**Fig. 10. Motile microorganisms density profile for various $Sc$.**

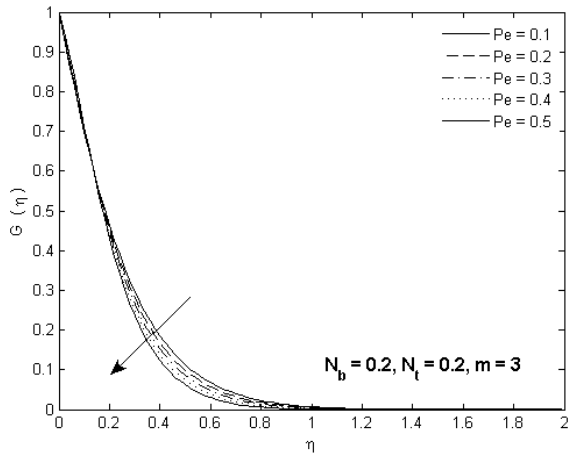


**Fig. 11. Motile microorganisms density profile for various $Pe$.**

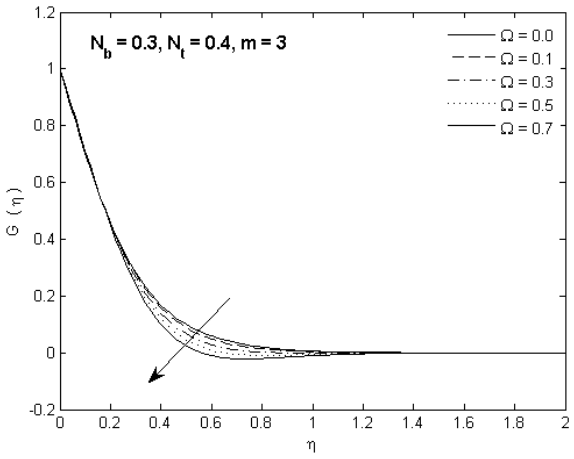


**Fig. 12. Motile microorganisms density profile for various $\Omega$.**

Figures 8 and 9 are drawn against the concentration distribution for multiple values of the Brownian motion parameter and the Lewis number. The effect of these two parameters is to downturn the concentration profiles. The behavior of the motile microorganism density profiles for the distinct values of the bioconvection Schmidt number, Peclet number and the microorganism concentration difference parameter have been scrutinized in figs. 10-12. The microorganisms concentration profiles fall with escalating values of $Sc$, $Pe$ and $\Omega$. The cell swimming $W_c$ is directly proportional to $Pe$ (Peclet number) and inversely proportional to $D_n$ (diffusivity of microorganisms). It is observed here that the effect of $N_t$ significantly increases the temperature profile and consequently the thickness of the thermal boundary layer enhances while the effect of $N_b$ tends to decrease the concentration profile.

## Conclusions

A comprehensive numerical investigation of the nanofluid dynamics through a porous medium taking into account the effects of gyrotactic microbes is introduced. Successive over Relaxation Parameter (SOR) method is employed to acquire the numerical solution against concentration, thermal energy, motile microorganism density and velocity. The major findings of this article are mentioned below:

- Porous medium enhances the shear stress as well as the flow.
- The enhancement in $S_c$ causes an increase in microorganisms' diffusion rate while it declines the density profile.
- The large estimations of Peclet number are linked with low diffusivity of microorganisms that causes the reduction in motile microorganisms density profile.
- The Lewis number enhances the mass transfer and the thermophoresis parameter reduces the heat transfer rate.

**Nomenclature**

$k^*$ Darcy permeability, $\left[NA^{-2}\right]$

$N$ Microorganism concentration, $\left[mol/m^3\right]$

$T_\infty$ Ambient temperature, $\left[K\right]$

$T$ Temperature, $\left[K\right]$

$W_c$ Cell swimming speed, $\left[ms^{-1}\right]$

$C$ Concentration of fluid, $\left[mol/m^3\right]$

$\tau$ Nanofluid heat capacity, $\left[J/kg\right]$

$C_\infty$ Ambient concentration, $\left[-\right]$

$D_B$ Brownian diffusion coefficient, $\left[m^2s^{-1}\right]$

$D_n$ Diffusivity of microorganisms, $\left[m^2s^{-1}\right]$

$D_T$ Thermophoretic coefficient, $\left[MLT^{-3}\theta^{-1}\right]$

**Greek Symbols**

$\rho$ Fluid density, $[kgm^{-3}]$

$\mu$ Dynamic viscosity, $[Nsm^{-2}]$

$\eta$ Similarity variable, $\left[-\right]$

$\theta$ Dimensionless temperature, $\left[-\right]$

$\upsilon$ Kinematics viscosity, $[m^2s^{-1}]$

$\tilde{\beta}$ Thermal conductivity, $[Wm^{-1}K^{-1}]$

**Acknowledgements**

The authors wish to express their sincere thanks to the honorable editor and referees for their valuable comments to improve the quality of the paper.

## References

[1] Mutuku, W. N., Makinde, O. D., Hydromagnetic bioconvection of nanofluid over a permeable vertical plate due to gyrotactic microorganisms, *Comput. Fluids*., 95 (2014), pp. 88–97

[2] Md. Tausif, S. K., Kalidas, D., Kundu, P. K., Multiple slip effects on bioconvection of nanofluid flow containing gyrotactic microorganisms and nanoparticles, *J. Mol.Liq.* 220 (2016), pp. 518–526

[3] Acharya, N., Kalidas, D., Kundu, P. K., Framing the effects of solar radiation on magneto-hydrodynamics bioconvection nanofluid flow in presence of gyrotactic microorganisms, *J.Mol. Liq.*, 222 (2016), pp. 28–37

[4] El Gamal, A. A., Biological importance of marine algae, *Saudi Phar. J.* 18 (2010), pp. 1-25 https://doi.org/10.1016/j.jsps.2009.12.001

[5] Khan, W. A., Makinde, O. D., Khan, Z. H., MHD boundary layer flow of a nanofluid containing gyrotactic microorganisms past a vertical plate with Navier slip, *Int. J. Heat Mass Transf.*, 74 (2014), pp. 285–291

[6] Stewart, T. L., Fogler, H. S., Biomass plug development and propagation in porous media, *Biotech. Bioeng.* 72 (2001), pp. 353–363

[7] Kuznetsov, A. V., The onset of nanofluid bioconvection in a suspension containing both nanoparticles and gyrotactic microorganisms, *Int. Commun. Heat Mass Transfer*, 37 (2010), pp. 1421–1425

[8] Ramzan M, Chung J D, Naeem U., Radiative magnetohydrodynamic nanofluid flow due to gyrotactic microorganisms with chemical reaction and non-linear thermal radiation, *I. J. Mech Sci.*, (2017), 130, pp. 31–40

[9] Chakraborty, T., Kalidas, D., Kundu, P. K., Framing the impact of external magnetic field on bioconvection of a nanofluid flow containing gyrotactic microorganisms with convective boundary conditions, *Alexandria Engg. J.*, 57 (2018), pp. 61–71

[10] Rashidi, M. M., Ghahremanian, S., Toghraie, D., Roy, P., Effect of solid surface structure on the condensation flow of Argon in rough nanochannels with different roughness geometries using molecular dynamics simulation, Int. Commu. Heat Mass Transf., 117 (2020), 104741 https://doi.org/10.1016/j.icheatmasstransfer.2020.104741

[11] Rashad, A. M., Rashidi, M. M., Lorenzini, G., Ahmed, S. E., Aly, A. M., Magnetic field and internal heat generation effects on the free convection in a rectangular cavity filled with a porous medium saturated with Cu–water nanofluid. International Journal of Heat and Mass Transfer, 104 (2017), pp. 878–889. doi:10.1016/j.ijheatmasstransfer.2016.08.025

[12] Alsaedi, A., Ijaz, K. M., Farooq, M., Gull, N., Hayat, T., Magnetohydrodynamic (MHD) stratified bioconvective flow of nanofluid due to gyrotactic microorganisms. *Advanced Powder Technology* 28 (2017), pp. 288–298

[13] Shahid, A., Zhou1, Z., Bhatti, M. M., Tripathi, D., Magnetohydrodynamics nanofluid flow containing gyrotactic microorganisms propagating over a stretching surface by Successive Taylor Series Linearization Method, *Microgravity Sci. Technol*., 30 (2018), 4, pp. 445–455 https://doi.org/10.1007/s12217-018-9600-2

[14] Aziz, A., Khan, W. A., Pop, I., Free convection boundary layer flow past a horizontal flat plate embedded in porous medium filled by nano-fluid containing gyrotactic microorganisms, *Int. J. Therm. Sci.*, 56 (2012), pp. 48

[15] Mohebbi, R., Rashidi, M. M., Numerical simulation of natural convection heat transfer of a nanofluid in an L-shaped enclosure with a heating obstacle. Journal of the Taiwan Institute of Chemical Engineers, 72, (2017), pp. 70–84. doi:10.1016/j.jtice.2017.01.006

[16] Shen, B., Zheng, I., Zhang, c., Zhang, x., Bioconvection heat transfer of a nanofluid over a stretching sheet with velocity slip and temperature jump, *Thermal Science.*, 21 (2017), 6A, pp. 2347-2356

[17] Ahmad, S., Ashraf, M., Ali, K., Simulation of thermal radiation in a micropolar fluid flow through a porous medium between channel walls, *J. Therm. Anal. Calorim.*, (2020) https://doi.org/10.1007/s10973-020-09542-w

[18] Ahmad, S., Ashraf, M., Ali, K., (2020). Heat and mass transfer flow of gyrotactic microorganisms and nanoparticles through a porous medium, *Int. J. Heat Tech.*, 38 (2020), pp. 395-402

[19] Ahmad, S., Ashraf, M., Ali, K., Numerical simulation of viscous dissipation in a micropolar fluid flow through a porous medium, *J. Appl. Mech. Tech. Phys.*, 60 (2019), 996–1004

[20] Ahmad, S., Ashraf, M., Ali, K., Nanofluid flow comprising gyrotactic microorganisms through a porous medium, *JAFM*., 13 (2020), pp. 1539-1549

[21] Ashraf, M., Kamal, M.A., Syed, K.S., Numerical simulation of a micropolar fluid between a porous disk and a non-porous disk, App. Math. Model., 33 (2009), pp. 1933-1943

[22] Ashraf, M., Kamal, M.A., Syed, K.S., Numerical simulation of flow of micropolar fluids in a channel with a porous wall, Int. J. Numer. Meth. Fl., 66 (2011), pp. 906-918

[23] Ahmad, S., Ashraf,M., Ali, K., Micropolar Fluid Flow with Heat Generation through a Porous Medium, *PUJM.*, 52(4) (2020), pp. 101-113.

[24] Hildebrand, F. B., Introduction to Numerical Analysis. *Tata McGraw-Hill Publishing Company: New Delhi,* (1978)

[25] Rashidi, M. M., Vishnu Ganesh, N., Abdul Hakeem, A. K., Ganga, B., Buoyancy effect on MHD flow of nanofluid over a stretching sheet in the presence of thermal radiation. *J. Mol. Liq.,* 198 (2014), 234–238 doi:10.1016/j.molliq.2014.06.037

Submitted: 07.12.2019.
Revised: 26.09.2020.
Accepted: 16.10.2020.